Am J Cancer Res 2019;9(1):36-52
www.ajcr.us /ISSN:2156-6976/ajcr0088433

Original Article

microRNA-758 inhibits the malignant phenotype of osteosarcoma cells by directly targeting *HMGA1* and deactivating the Wnt/β-catenin pathway

Jia Ren[1], Mengjie Yang[2], Fengyang Xu[1], Juwu Chen[1]

[1]*Department of Emergency, The First Affiliated Hospital of Zhengzhou University, Henan 450052, P. R. China;* [2]*National Institute for Viral Disease Control and Prevention, Chinese Center for Disease Control and Prevention, Beijing 102206, P. R. China*

Received November 15, 2018; Accepted December 28, 2018; Epub January 1, 2019; Published January 15, 2019

Abstract: microRNAs (miRNAs) are frequently aberrantly expressed in osteosarcoma (OS) and are implicated in its development. Dysregulation of miR-758 has been reported in various human malignancies. However, whether miR-758 is involved in the oncogenesis and progression of OS remains unclear. In this study, reverse transcription-quantitative polymerase chain reaction was performed to detect miR-758 expression in OS tissues and cell lines. A series of functional experiments were employed to explore the regulatory effects of miR-758 on the malignant behaviors of OS cells both in vitro and in vivo. The molecular mechanisms underlying the activity of miR-758 in OS cells were also investigated. miR-758 was significantly downregulated in OS tissues and cell lines, and a low miR-758 level was correlated with tumor size, clinical stage, and distant metastasis of patients with OS. OS patients with low miR-758 level exhibited poorer overall survival and worse disease-free survival rates compared to patients with high miR-758 level. In addition, functional assays revealed that miR-758 overexpression led to a significant decrease in OS cell growth and metastasis in vitro, whereas miR-758 inhibition had the opposite effect on OS cells. miR-758 reduced the tumorous growth of OS cells in vivo. Furthermore, high mobility group AT-hook 1 (*HMGA1*) was identified as a direct target of miR-758 in OS cells. *HMGA1* was highly expressed in OS tissues, and its expression was inversely correlated with miR-758 expression. *HMGA1* silencing exerted an effect similar to that induced by miR-758 upregulation in OS cells. Restored *HMGA1* expression abolished the effects of miR-758 on the malignant phenotypes of OS cells. Moreover, miR-758 regulated the Wnt/β-catenin pathway in OS cells in vitro and in vivo. To the best of our knowledge, this is the first study to demonstrate that miR-758 may inhibit the aggressive behavior of OS cells in vitro and in vivo by directly targeting *HMGA1* and regulating the Wnt/β-catenin pathway. These results will aid in elucidating the roles of miR-758 and suggest that the miR-758/HMGA1/Wnt/β-catenin pathway represents a potential therapeutic target in OS.

Keywords: High mobility group AT-hook 1, malignant phenotype, microRNA-758, osteosarcoma, Wnt/β-catenin pathway

Introduction

Osteosarcoma (OS), derived from the mesenchymal tissue, is a common primary bone malignancy in adolescents and children [1]. OS can occur in any bone in the body, but it mainly occurs in the metaphysis of long bones [2]. Currently, primary chemotherapy in combination with surgical resection and adjuvant chemotherapy are the predominant treatments for patients with OS [3]. Despite considerable progress in diagnosis and therapy, the efficacy of OS treatment remains unsatisfactory, especially for patients diagnosed at advanced stages of the disease [4, 5]. Several factors, such as ionizing radiation, alkylating agents, Paget's disease, and Li-Fraumeni familial cancer syndrome have been demonstrated to be involved in the genesis and development of OS [6]. However, the molecular events characterizing the pathogenesis of OS remain obscure. Therefore, investigating the mechanisms that contribute to the carcinogenesis and development of OS is essential for developing novel

therapeutic approaches and improving the prognosis and outcome of patients with this malignancy.

microRNAs (miRNAs) are 19-23 nucleotide-long endogenous, non-coding short RNA molecules [7], which regulate gene expression by hybridizing completely or incompletely with the 3'-untranslated regions (3'-UTRs) of their target genes [8]. These interactions inhibit the translation of the targeted genes or induce their degradation [9]. In total, over 1,500 mature miRNAs have been identified in the human genome, which are estimated to regulate approximately 50% of all human protein-coding genes [10]. Alterations in miRNA expression have been reported in almost all human cancer types, including OS [11]. Currently, several miRNAs, such as miR-216b [12], miR-337 [13], and miR-130 [14] have been shown to be aberrantly expressed in OS and are closely-associated with the malignant progression of OS [15]. Hence, investigations regarding OS-related miRNAs may aid in the identification of therapeutic targets for future diagnosis, therapy, and prognosis of patients with this aggressive malignancy.

Dysregulation of miR-758 has been reported in various human malignancies [16-19]. However, whether miR-758 is involved in the oncogenesis and progression of OS remains unclear. In this study, we demonstrated for the first time that miR-758 is aberrantly expressed in OS tissues and cell lines. Simultaneously, the association between miR-758 expression and clinicopathological features, as well as prognosis of patients with OS was determined. Gain- and loss-of-function studies were performed to investigate the effects of miR-758 on the regulation of OS cell biology. Furthermore, the molecular mechanisms underlying the action of miR-758 in OS cells were determined.

Material and methods

Patients and tissue samples

In total, 53 pairs of OS tissues and corresponding adjacent non-cancer tissues were collected from patients at The First Affiliated Hospital of Zhengzhou University between July 2015 and August 2017. None of the patients had been treated with radiotherapy or chemotherapy prior to surgery. All tissues were rapidly frozen in liquid nitrogen and then stored at -80°C for further experiments. Our current study was approved by the Ethics Committee of The First Affiliated Hospital of Zhengzhou University. All patients provided written informed consent prior to surgical resection.

Cell lines and culture conditions

Three human OS cell lines, including HOS, U2OS, and MG-63, and a normal human osteoblast line hFOB1.19, were purchased from American Type Culture Collection (Manassas, VA, USA). All cell lines were cultured in Dulbecco's modified Eagle's medium (DMEM) containing 10% fetal bovine serum (FBS; both from Gibco, Invitrogen, Carlsbad, CA, USA), 100 units/ml penicillin, and 100 mg/ml streptomycin (both from Sigma-Aldrich, Merck KGaA, Darmstadt, Germany). All cultures were maintained in a humidified atmosphere with 5% CO_2 at 37°C.

Cell transfection

miR-758 mimics, miR-758 inhibitor, negative control miRNA mimics (miR-NC), and negative control RNA inhibitor (NC inhibitor) were purchased from GenePharma (Shanghai, China). Small interfering RNA (siRNA) used for *HMGA1* knockdown (*HMGA1* siRNA) and negative control siRNA (NC siRNA) were obtained from RiboBio (Guangzhou, China). For *HMGA1* overexpression, a full-length human *HMGA1* cDNA lacking its 3'-UTR was amplified by the Chinese Academy of Sciences (Changchun, China) and inserted into the pcDNA3.1 (+) plasmid (Invitrogen, Carlsbad, CA, USA). The chemically synthesized plasmid was defined as pcDNA3.1-HMGA1 (pc-HMGA1). For transfection, cells in the logarithmic growth phase were harvested and seeded into 6-well plates one day before the transfection. Cell transfection was performed using Lipofectamine 2000 (Invitrogen, Thermo Fisher Scientific, Inc., Waltham, MA, USA) according to the manufacturer's recommendation. The transfected cells were collected at different time points for further analysis.

Reverse transcription-quantitative polymerase chain reaction (RT-qPCR)

The levels of miR-758 and *HMGA1* mRNA were detected using RT-qPCR. First, transfected cells were collected after 48 h of incubation.

Total RNA was extracted from tissue specimens or cells using TRIzol reagent (Invitrogen, Thermo Fisher Scientific, Inc., Waltham, MA, USA) according to the manufacturer's protocol. The All-in-One™ miRNA qRT-PCR detection kit (GeneCopoeia, Rockville, MD, USA) was used to determine miR-758 expression. The thermocycling conditions were as follows: 95°C for 10 min, followed by 45 cycles of denaturation at 95°C for 15 sec and annealing/elongation at 60°C for 15 sec. To quantify *HMGA1* mRNA level, total RNA was used for reverse transcription to generate complementary DNA using PrimeScript RT reagent kit (Takara, Dalian, China). The temperature conditions for reverse transcription were as follows: 37°C for 15 min and 85°C for 5 sec. PCR amplification was performed using a SYBR premix Ex Taq™ kit (Takara Bio, Dalian, China). The thermocycling conditions for PCR amplification were as follows: 5 min at 95°C, followed by 40 cycles of 95°C for 30 sec and 65°C for 45 sec. All RT-qPCR reactions were performed on the ABI 7900 sequence detection system (Applied Biosystems, Thermo Fisher Scientific, Inc., Waltham, MA, USA). miR-758 expression was normalized to that of U6 small nuclear RNA, whereas *HMGA1* expression was normalized to that of glyceraldehyde phosphate dehydrogenase (*GAPDH*). The primers were designed as follows: miR-758, 5'-ACACTCCAGCTGGGTTTGTGACCTGGTCCA-3' (forward) and 5'-TGGTGTCGTGGAGTCG-3' (reverse); U6, 5'-CGCTTCGGCAGCACATATACTA-3' (forward) and 5'-GCGAGCACAGAATTAATACGAC-3' (reverse); *HMGA1*, 5'-GAAGGTGAAGGTCGGAGTC-3' (forward) and 5'-GAAGATGGTGATGGGATTTC-3' (reverse); and GAPDH, 5'-GGCACTGAGAAGCGGGGCCG-3' (forward) and 5'-CCCTTGTTTTTTGCTTCCCTT-3' (reverse). Relative gene expression was calculated using the $2^{-\Delta\Delta Cq}$ method [20].

3-(4,5-dimethylthiazol-2-yl)-2,5-diphenyltetrazolium bromide (MTT) assay

Twenty-four hours post-transfection, cells were harvested, re-suspended, and plated into 96-well plates with a density of 2×10^3 cells per well. After different time points, MTT assay was performed to evaluate cellular proliferation. Briefly, 20 μL MTT reagent (5 mg/ml; Sigma-Aldrich, Merck KGaA, Darmstadt, Germany) was added to every well prior to incubation at 37°C for another 4 h. Next, the supernatant was removed and 200 μl dimethyl sulfoxide was added into each well. The absorbance was detected at 490 nm using a Victor 3 multilabel microplate reader (PerkinElmer, Inc., Waltham, MA, USA).

Clonogenic survival assay

Transfected cells were collected, counted, and inoculated into 6-well plates at a density of 1×10^3 cells/well. Cells were incubated at 37°C in a humidified atmosphere supplied with 5% CO_2. After 14 days of culture, the colonies were washed with phosphate buffered solution (PBS; Gibco, Invitrogen, Carlsbad, CA, USA), fixed with 4% paraformaldehyde, and stained with methyl violet (Beyotime Institute of Biotechnology, Haimen, China). The number of colonies was counted under an IX83 Olympus inverted light microscope (Olympus, Tokyo, Japan).

Flow cytometry analysis

Forty-eight hours after incubation, the transfected cells were dissociated using trypsin and washed with PBS. Next, the cell apoptosis rate was determined using an annexin V fluorescein isothiocyanate (FITC) apoptosis detection kit (BioLegend, San Diego, CA, USA). Briefly, transfected cells were suspended into 100 μl of 1 × binding buffer. Subsequently, 5 μl each of annexin V-FITC and propidium iodide (PI) were added into the cell suspension, mixed carefully, and incubated at room temperature in the dark for 15 min. The percentage of apoptotic cells was assessed using a flow cytometer (FACScan™; BD Biosciences, Franklin Lakes, NJ, USA). Cell Quest software 5.1 (BD Biosciences) was used to analyze the data.

Transwell assay

Transwell chambers (Corning Incorporated, Corning, NY, USA) with or without Matrigel (BD Biosciences, San Jose, CA, USA) were used to determine invasion and migration of OS cells, respectively. Forty-eight hours post-transfection, cells were collected and resuspended in FBS-free DMEM. In total, 5×10^4 cells/200 μl suspension were plated onto the upper compartments of chambers. At the same time, 500 μl of DMEM supplemented with 20% FBS was added to the lower compartments to act as a chemoattractant. Cells remaining on the upper chambers were gently removed with a cotton swab. Cells adhering to the lower surface of the chambers were fixed with 4% paraformalde-

hyde and stained with 0.05% crystal violet. Finally, the number of invasive and migratory cells in five random fields of view was counted under an IX83 Olympus inverted light microscope.

Xenograft assay

Six-week-old nude mice were obtained from the Chinese Academy of Sciences (Shanghai, China). miR-758 mimics or miR-NC was transfected into cells. After 24 h of incubation, cells were collected and subcutaneously injected into the flanks of nude mice. Two weeks after the transplantation, the width and length of the xenograft formed were measured using Vernier calipers and the tumor volume was calculated using the following formula: Volume (mm^3) = Width^2 (mm^2) * Length (mm)/2. All nude mice were sacrificed one month after injection. The tumor xenografts were separated and weighed. The procedures for care and use of animals were approved by the Ethics Committee of The First Affiliated Hospital of Zhengzhou University, and all applicable institutional and government regulations concerning the ethical use of animals were followed.

Bioinformatics analysis

The potential targets of miR-758 were predicted using TargetScan Human 7.1 (http://www.targetscan.org/vert_71/) and mirTarBase (http://mirtarbase.mbc.nctu.edu.tw/php/index.php).

Luciferase reporter assay

The 3'-UTR region of human *HMGA1* containing the wild-type (WT) or mutant (MUT) miR-758 binding site was chemically synthesized by GenePharma. These fragments were inserted into a pmirGLO Dual-luciferase target vector (Promega Corporation, Madison, WI, USA) to generate the recombinant luciferase reporter plasmids, pmirGLO-HMGA1-3'-UTR-WT and pmirGLO-HMGA1-3'-UTR-MUT. For the reporter assay, cells were plated into 24-well plates one night prior to the transfection. The recombinant luciferase reporter plasmids along with either miR-758 mimics or miR-758 inhibitor were co-transfected into cells using Lipofectamine 2000. Forty-eight hours post-transfection, the transfected cells were collected using trypsin and luciferase activity was detected using a dual-luciferase reporter assay system (Promega Corporation, Madison, WI, USA). Firefly luciferase activity was normalized against that of Renilla luciferase.

Western blot analysis

Homogenized tissues or cells were lysed in radioimmunoprecipitation assay buffer (Thermo Fisher Scientific, Inc., Waltham, MA, USA) containing a protease inhibitor (Sigma-Aldrich, Merck KGaA, Darmstadt, Germany). A bicinchoninic acid protein assay kit (Pierce; Thermo Fisher Scientific, Inc., Waltham, MA, USA) was used to evaluate the protein concentration. Equal amounts of protein were loaded for sodium dodecyl sulfate-polyacrylamide gel electrophoresis on 10% polyacrylamide gels, followed by transfer to polyvinylidene difluoride membranes (Beyotime Institute of Biotechnology, Haimen, China). Subsequently, the membranes were blocked in 5% dried skimmed milk diluted in TBS containing 0.1% Tween-20 (TBST) at room temperature for 2 h. Following overnight incubation at 4°C with primary antibodies, the membranes were washed thrice with TBST and further treated with corresponding horseradish peroxidase-conjugated secondary antibody (ab6721 and ab205719; 1:5000 dilution; Abcam, Cambridge, UK) at room temperature for 1 h. Immunoblotting was performed using an enhanced chemiluminescence (ECL) protein detection kit (Pierce, Thermo Fisher Scientific, Inc., Waltham, MA, USA). The primary antibodies used were as follows: rabbit anti-human monoclonal HMGA1 (ab129153; 1:1000 dilution; Abcam, Cambridge, UK), mouse anti-human monoclonal β-catenin (sc-59737; 1:1000 dilution; Santa Cruz Biotechnology, CA, USA), mouse anti-human monoclonal p-β-catenin (sc-57534; 1:1000 dilution; Santa Cruz Biotechnology, CA, USA), rabbit anti-human monoclonal cyclin D1 (ab134175; 1:1000 dilution; Abcam, Cambridge, UK), and rabbit anti-human GAPDH (ab181603; 1:1000 dilution; Abcam, Cambridge, UK). The signals from target proteins were normalized to those of GAPDH.

Statistical analysis

All data are shown as the mean ± standard deviation (SD) from three independent experiments. Student's *t*-test and one-way analysis of variance (ANOVA) were used to analyze differences between two groups and multiple groups, respectively. Tukey's test was used for post hoc

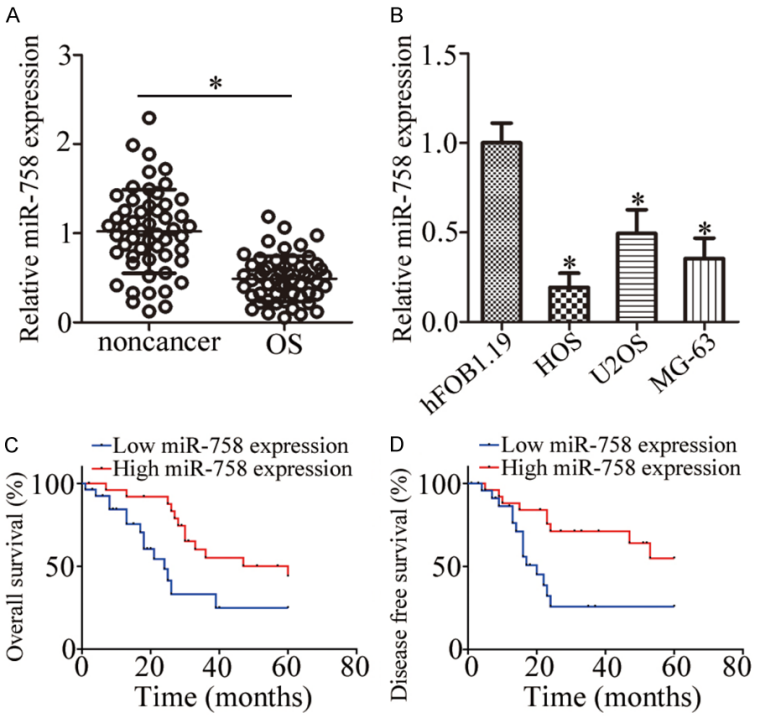

Figure 1. miR-758 is downregulated in OS tissues and cell lines. A. miR-758 expression was assessed in 53 pairs of OS tissues and corresponding adjacent non-cancer tissues using RT-qPCR. **P* < 0.05 vs. non-cancer tissues. B. RT-qPCR was used for the determination of miR-758 expression in three human OS cell lines (HOS, U2OS, and MG-63) and a normal human osteoblast hFOB1.19. **P* < 0.05 vs. hFOB1.19. C, D. The overall and disease-free survival of OS patients with low or high miR-758 expression were determined using Log-rank test.

analysis following ANOVA. The correlation between miR-758 expression and clinicopathological variables of patients with OS was investigated using chi-square test. The Kaplan-Meier survival analysis was used to determine survival rate and Log-rank test was used to assess the association between miR-758 levels and overall survival as well as disease-free survival. Spearman's correlation analysis was used to determine the association between miR-758 and *HMGA1* mRNA level in OS tissues. All statistical analyses were performed using SPSS 20.0 software (IBM Corp., Armonk, NY, USA). *P* < 0.05 was considered statistically significant.

Results

miR-758 is downregulated in OS and correlated with poor prognosis in patients with OS

To investigate the expression pattern of miR-758 in OS, we determined miR-758 level in 53 pairs of OS tissues and corresponding adjacent non-cancer tissues. Results indicated that miR-758 expression was lower in OS tissues than that in adjacent non-cancer tissues (**Figure 1A**, *P* < 0.05). In addition, we determined miR-758 expression in three human OS cell lines, HOS, U2OS, and MG-63, using the normal human osteoblast hFOB1.19 as a control. RT-qPCR revealed that miR-758 expression was lower in all three OS cell lines than that in hFOB1.19 (**Figure 1B**, *P* < 0.05).

To determine the clinical significance of miR-758 in OS, we subsequently divided all enrolled patients into low or high miR-758 expression groups with the median value as a cutoff. Statistical analysis demonstrated that low miR-758 expression correlated significantly with tumor size (*P* = 0.019), clinical stage (*P* = 0.009), and distant metastasis (*P* = 0.004) of the patients (**Table 1**). Furthermore, OS patients with low miR-758 level showed poorer overall survival (**Figure 1C**, *P* = 0.013) and worse disease-free survival (**Figure 1D**, *P* = 0.007) than patients with high miR-758 level. These results suggest that miR-758 downregulation may contribute to the progression and development of OS.

miR-758 inhibits the malignant phenotypes of OS cells in vitro

According to **Figure 1B**, miR-758 expression was relatively lowest in HOS cells but highest in U2OS cells; therefore, these two cell lines were selected as models for subsequent functional experiments. HOS cells were transfected with miR-758 mimics or miR-NC, whereas U2OS cells were transfected with miR-758 inhibitor or NC inhibitor. RT-qPCR analysis verified that miR-758 expression was notably upregulated in miR-758 mimics-transfected HOS cells, but significantly downregulated in miR-758 inhibitor-transfected U2OS cells (**Figure 2A**, *P* < 0.05). MTT and clonogenic survival assays were per-

Table 1. Relationship between miR-758 expression and clinicopathological factors of patients with OS

Factors	miR-758 expression		*P*
	Low	High	
Age (years)			0.215
< 20	19	22	
≥ 20	8	4	
Gender			0.328
Male	13	16	
Female	14	10	
Tumor size (cm)			0.019*
< 5	10	18	
≥ 5	17	8	
Clinical stage			0.009*
I-IIA	8	17	
IIB/III	19	9	
Distant metastasis			0.004*
Negative	9	19	
Positive	18	7	

*$P < 0.05$.

formed to determine the effect of miR-758 on OS cell proliferation. Results showed that miR-758 overexpression in HOS cells suppressed the proliferative capacity, which, however, was enhanced by miR-758 knockdown in U2OS cells (**Figure 2B** and **2C**, $P < 0.05$). Flow cytometry analysis was used to further confirm whether miR-758 affected cell proliferation by promoting apoptosis. We observed that the percentage of apoptosis in miR-758 mimics-transfected HOS cells was higher than that in miR-NC-transfected cells; the apoptosis rate was lower in U2OS cells treated with miR-758 inhibitor (**Figure 2D**, $P < 0.05$). Furthermore, transwell assays were used to determine the effect of miR-758 on OS cell metastasis in vitro. Results showed that cell migration and invasion were restricted in HOS cells after miR-758 overexpression. On the contrary, downregulation of miR-758 promoted migration and invasion of U2OS cells (**Figure 2E** and **2F**, $P < 0.05$). These observations suggested that miR-758 might play a tumor suppressive role in the growth and metastasis of OS cells in vitro.

HMGA1 is a direct target of miR-758 in OS cells

Considering the importance of miR-758 in the malignant development of OS, we next attempted to identify the direct targets of this miRNA. Bioinformatics analysis was used to identify the putative targets of miR-758. *HMGA1*, which was predicted as the potential target of miR-758 (**Figure 3A**), attracted our attention, as this gene is closely related to tumorigenesis and tumor development [21-25]. Luciferase reporter assay was performed to determine whether miR-758 directly interacts with the 3'-UTR of *HMGA1*. Transfection with miR-758 mimics reduced the luciferase activity of the plasmid that harbored the predicted wild-type miR-758 binding site in HOS cells, whereas transfection with miR-758 inhibitor increased its activity in U2OS cells ($P < 0.05$); however, mutation of miR-758-binding sequences in the 3'-UTR of *HMGA1* abrogated these effects on luciferase activity (**Figure 3B**).

We further analyzed *HMGA1* expression in OS tissues and explored its relationship with miR-758. The mRNA (**Figure 3C**, $P < 0.05$) and protein (**Figure 3D**, $P < 0.05$) levels of *HMGA1* in OS tissues were higher than those in adjacent non-cancer tissues. Furthermore, an inverse association between miR-758 and *HMGA1* mRNA levels in OS tissues was confirmed using Spearman's correlation analysis (**Figure 3E**; $r = -0.5380$, $P < 0.001$). In addition, we measured the *HMGA1* expression in HOS cells transfected with miR-758 mimics, as well as in U2OS cells transfected with miR-758 inhibitor. *HMGA1* expression at both mRNA (**Figure 3F**, $P < 0.05$) and protein (**Figure 3G**, $P < 0.05$) levels was inhibited by miR-758 overexpression in HOS cells and increased by miR-758 inhibition in U2OS cells, as demonstrated by RT-qPCR and western blot analysis. These results suggested that *HMGA1* is a direct target of miR-758 in OS cells.

Effects of HMGA1 silencing and miR-758 overexpression are similar in OS cells

We transfected HOS and U2OS cells with *HMGA1* siRNA or NC siRNA to investigate the biological function of *HMGA1* in OS cells. Western blot analysis showed that *HMGA1* expression was dramatically reduced in HOS and U2OS cells after *HMGA1* siRNA transfection (**Figure 4A**, $P < 0.05$). MTT and clonogenic survival assays were used to evaluate the proliferation ability of HOS and U2OS cells. Results showed that cell proliferation was remarkably

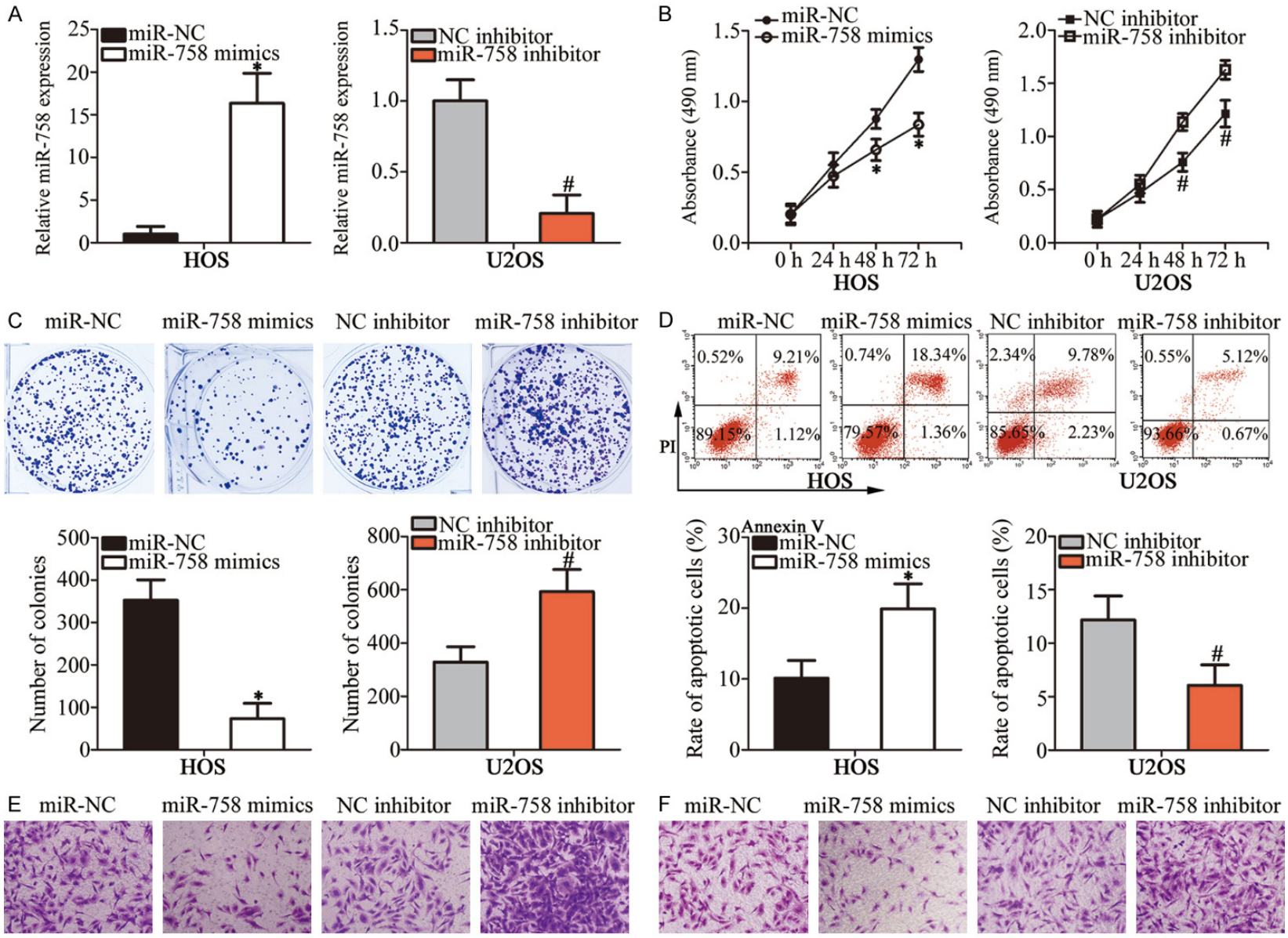
A
Relative miR-758 expression
miR-NC
miR-758 mimics
HOS
NC inhibitor
miR-758 inhibitor
U2OS
B
Absorbance (490 nm)
0 h 24 h 48 h 72 h
C
miR-NC
miR-758 mimics
NC inhibitor
miR-758 inhibitor
Number of colonies
D
0.52%
9.21%
89.15%
1.12%
0.74%
18.34%
79.57%
1.36%
2.34%
9.78%
85.65%
2.23%
0.55%
5.12%
93.66%
0.67%
PI
Annexin V
Rate of apoptotic cells (%)
E
F

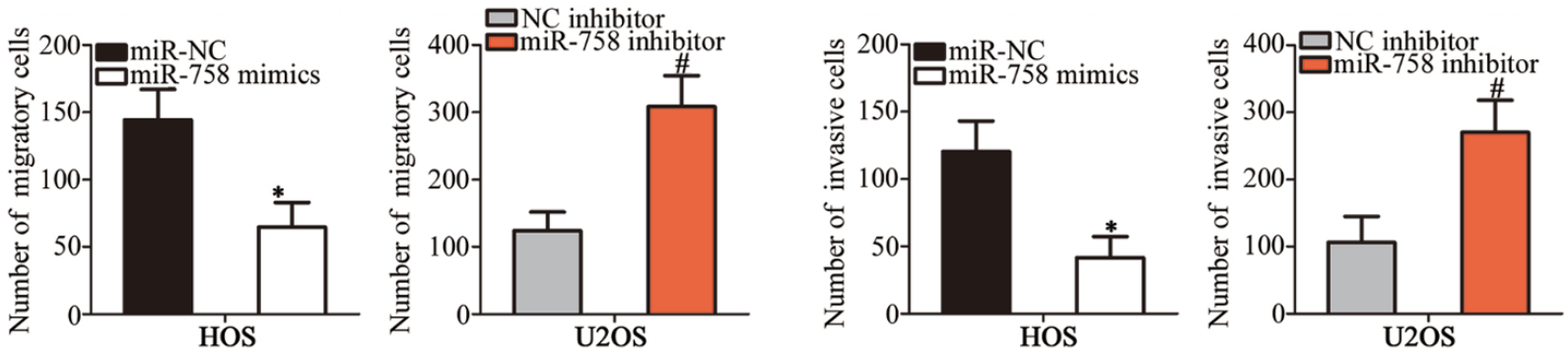

Figure 2. miR-758 inhibits proliferation, colony formation, migration, and invasion and induces apoptosis of OS cells in vitro. A. HOS and U2OS cells were transfected with miR-758 mimics and miR-758 inhibitor, respectively. RT-qPCR was performed at 48 h post-transfection to measure miR-758 expression. $^{*}P < 0.05$ vs. miR-NC. $^{\#}P < 0.05$ vs. NC inhibitor. B, C. The regulatory roles of miR-758 in OS cell proliferation and colony formation were evaluated using MTT and clonogenic survival assays, respectively. $^{*}P < 0.05$ vs. miR-NC. $^{\#}P < 0.05$ vs. NC inhibitor. D. Flow cytometry analysis to determine the effect of miR-758 on OS cell apoptosis. $^{*}P < 0.05$ vs. miR-NC. $^{\#}P < 0.05$ vs. NC inhibitor. E, F. Migration and invasion abilities of miR-758 mimics-transfected HOS and miR-758 inhibitor-transfected U2OS cells were determined using transwell assays. $^{*}P < 0.05$ vs. miR-NC. $^{\#}P < 0.05$ vs. NC inhibitor.

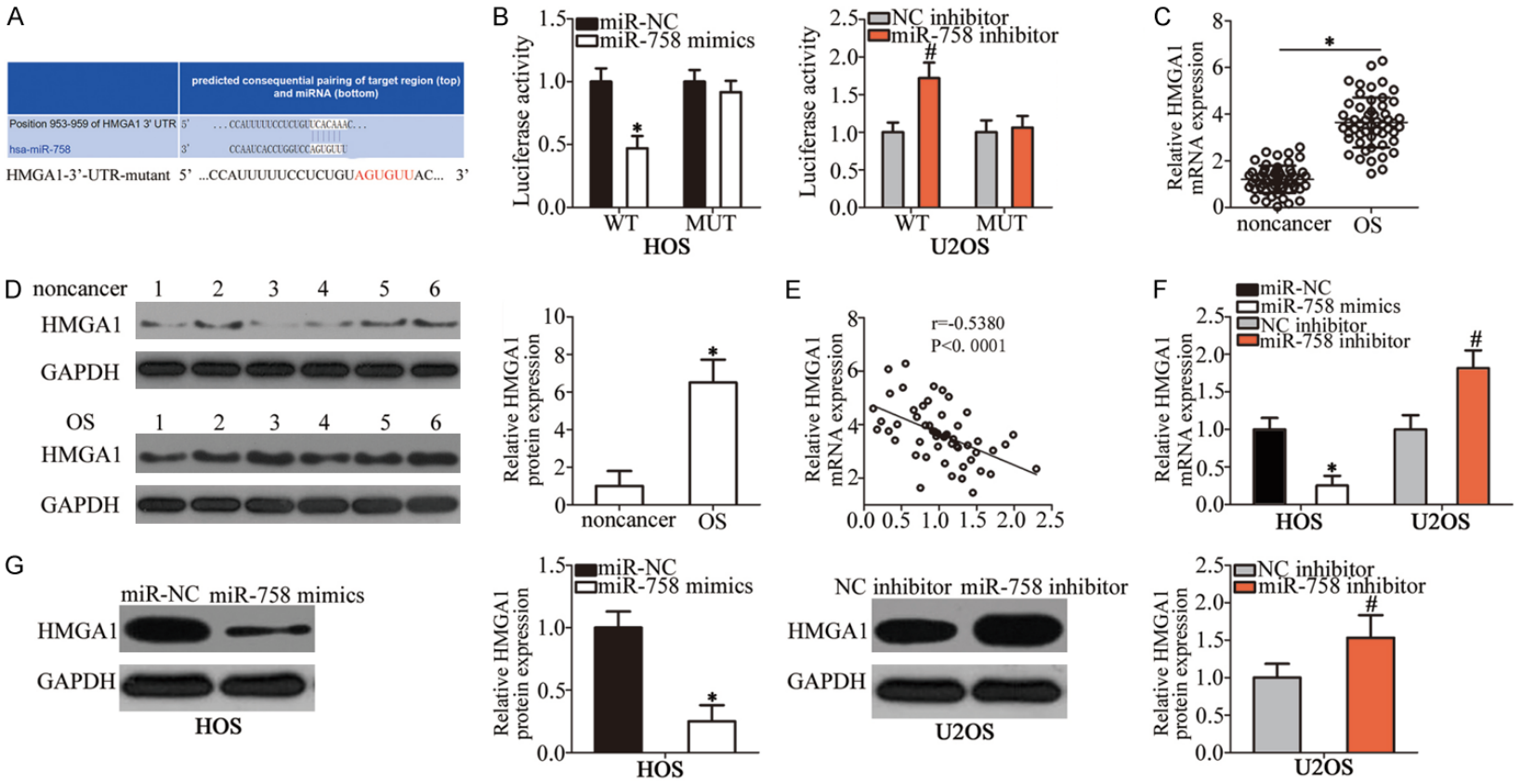

Figure 3. Identification of *HMGA1* as a direct target of miR-758 in OS cells. A. The binding site of miR-758 in the 3'-UTR of *HMGA1* was predicted using bioinformatics analysis. The mutant miR-758 binding sequences are also shown. B. HOS cells were co-transfected with miR-758 mimics or miR-NC and pmirGLO-HMGA1-3'-UTR-WT or pmirGLO-HMGA1-3'-UTR-MUT. miR-758 inhibitor or NC inhibitor was co-transfected with pmirGLO-HMGA1-3'-UTR-WT or pmirGLO-HMGA1-3'-UTR-MUT into U2OS cells. Luciferase activity was detected 48 h post-transfection to assess the binding between miR-758 and the 3'-UTR of *HMGA1*. $^{*}P < 0.05$ vs. miR-NC. $^{\#}P < 0.05$ vs. NC inhibitor. C, D. The mRNA and protein levels of *HMGA1* in OS tissues and corresponding adjacent non-cancer tissues were detected using RT-qPCR and western blot analysis, respectively. $^{*}P < 0.05$ vs. non-cancer tissues. E. Spearman's correlation analysis of the association between miR-758 and *HMGA1* mRNA levels in OS tissues. r = -0.5380, $P < 0.001$. F, G. RT-qPCR and western blot analysis results of *HMGA1* mRNA and protein levels in HOS and U2OS cells after transfection with miR-758 mimics and miR-758 inhibitor, respectively. $^{*}P < 0.05$ vs. miR-NC. $^{\#}P < 0.05$ vs. NC inhibitor.

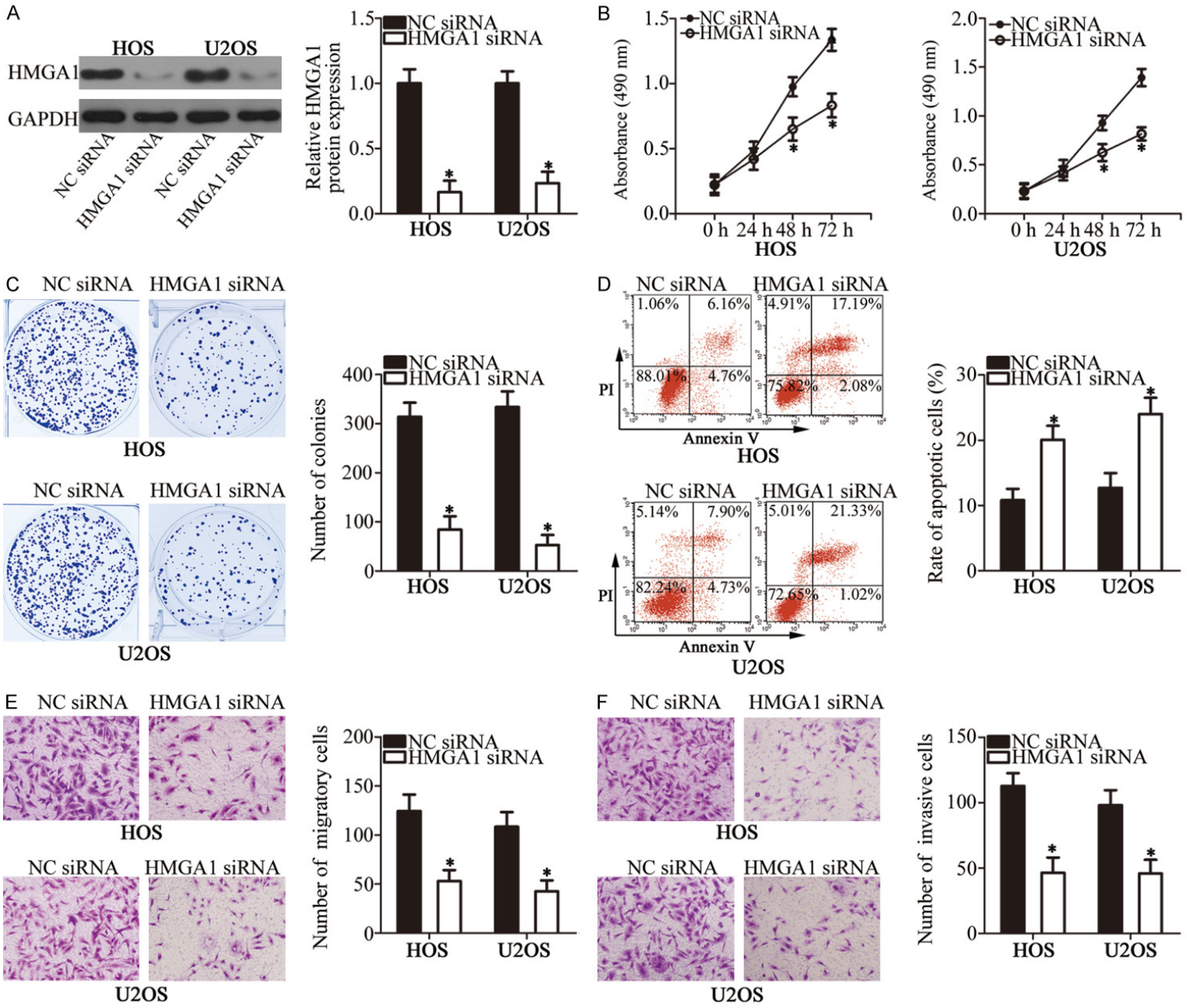
A
HOS
U2OS
HMGA1
GAPDH
NC siRNA
HMGA1 siRNA
NC siRNA
HMGA1 siRNA
Relative HMGA1 protein expression
NC siRNA
HMGA1 siRNA
HOS
U2OS
B
Absorbance (490 nm)
NC siRNA
HMGA1 siRNA
0 h 24 h 48 h 72 h
HOS
U2OS
C
NC siRNA
HMGA1 siRNA
HOS
U2OS
Number of colonies
D
1.06%
6.16%
88.01%
4.76%
4.91%
17.19%
75.82%
2.08%
5.14%
7.90%
82.24%
4.73%
5.01%
21.33%
72.65%
1.02%
PI
Annexin V
Rate of apoptotic cells (%)
E
F
Number of migratory cells
Number of invasive cells

Figure 4. *HMGA1* inhibition simulates the effects of miR-758 overexpression in OS cells. HOS and U2OS cells were transfected with *HMGA1* siRNA or NC siRNA. A. Western blot analysis was performed to determine HMGA1 protein level. **P* < 0.05 vs. NC siRNA. B, C. Proliferation and colony forming ability of the above-mentioned cells were investigated using MTT and clonogenic survival assays, respectively. **P* < 0.05 vs. NC siRNA. D. The percentage of apoptotic HOS and U2OS cells was detected using flow cytometry analysis. **P* < 0.05 vs. NC siRNA. E, F. Effects of *HMGA1* knockdown on the migratory and invasive abilities of HOS and U2OS cells were assessed using transwell assays. **P* < 0.05 vs. NC siRNA.

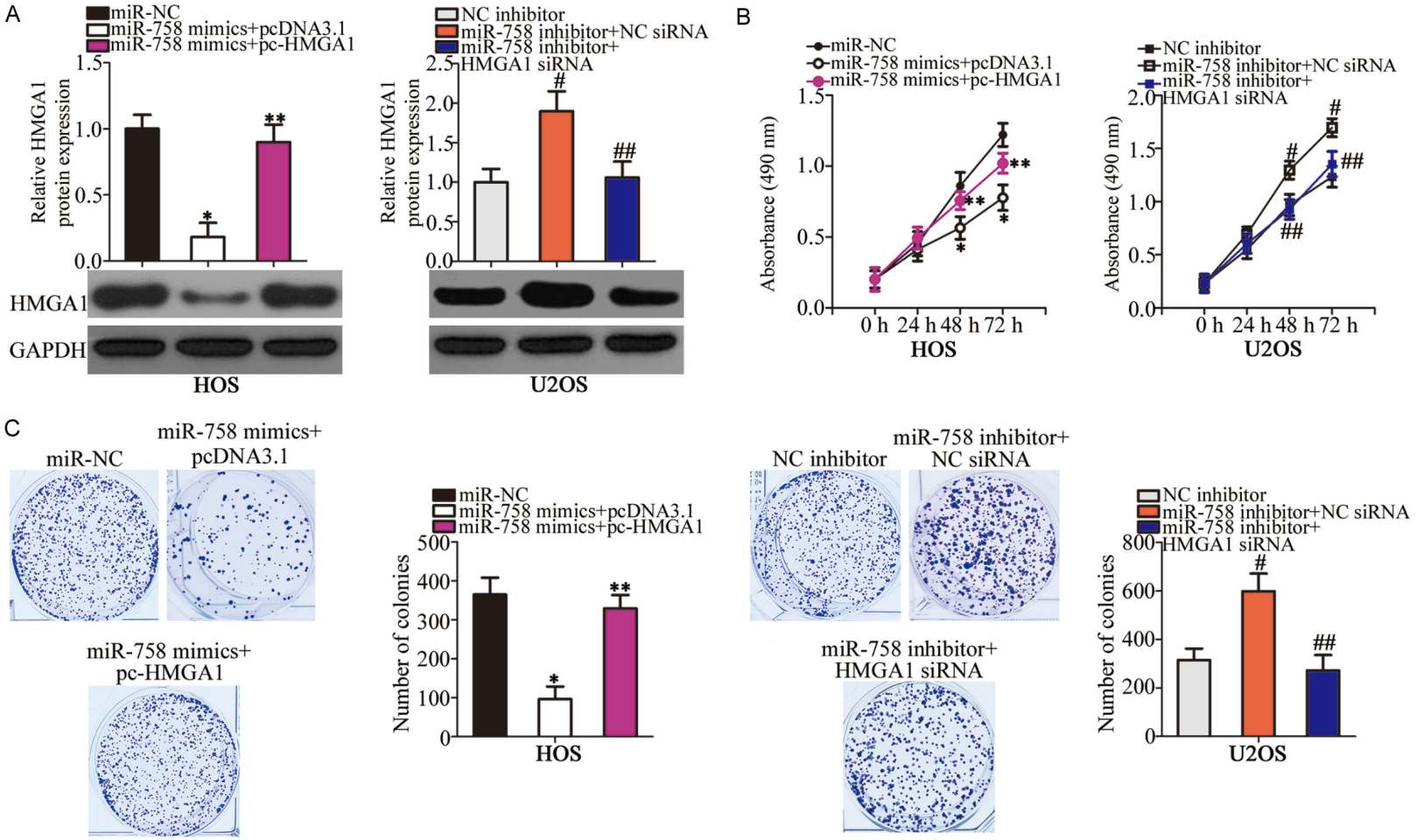

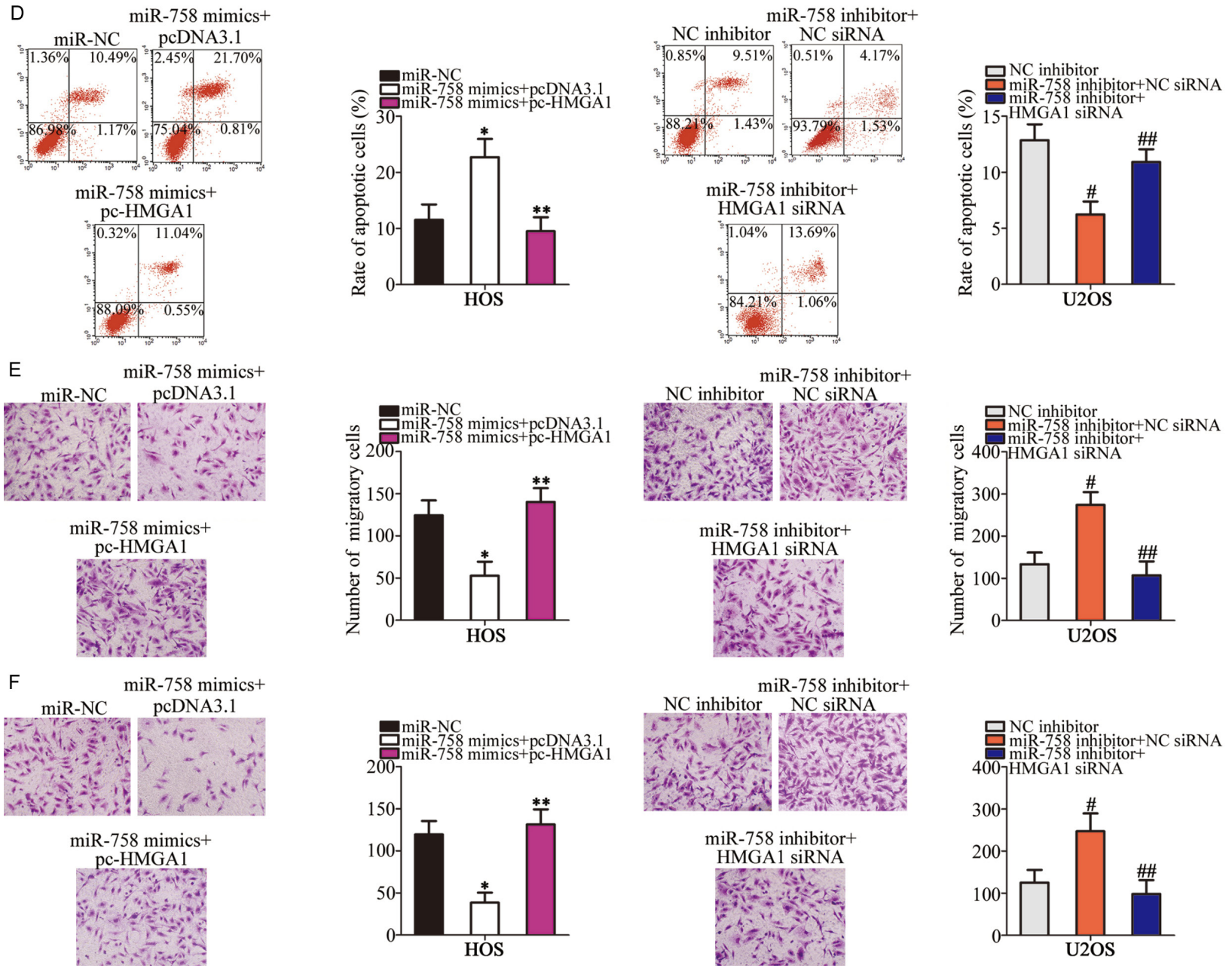
D
miR-NC
miR-758 mimics+ pcDNA3.1
1.36%
10.49%
86.98%
1.17%
2.45%
21.70%
75.04%
0.81%
miR-758 mimics+ pc-HMGA1
0.32%
11.04%
88.09%
0.55%
miR-NC
miR-758 mimics+pcDNA3.1
miR-758 mimics+pc-HMGA1
Rate of apoptotic cells (%)
HOS
miR-758 inhibitor+
NC inhibitor
NC siRNA
0.85%
9.51%
88.21%
1.43%
0.51%
4.17%
93.79%
1.53%
miR-758 inhibitor+ HMGA1 siRNA
1.04%
13.69%
84.21%
1.06%
NC inhibitor
miR-758 inhibitor+NC siRNA
miR-758 inhibitor+ HMGA1 siRNA
Rate of apoptotic cells (%)
U2OS
E
miR-NC
miR-758 mimics+ pcDNA3.1
miR-758 mimics+ pc-HMGA1
Number of migratory cells
HOS
miR-758 inhibitor+
NC inhibitor
NC siRNA
miR-758 inhibitor+ HMGA1 siRNA
U2OS
F
miR-NC
miR-758 mimics+ pcDNA3.1
miR-758 mimics+ pc-HMGA1
HOS
miR-758 inhibitor+
NC inhibitor
NC siRNA
miR-758 inhibitor+ HMGA1 siRNA
U2OS

Figure 5. HMGA1 is required for miR-758-directed OS cell proliferation, colony formation, apoptosis, migration, and invasion. miR-758-overexpressing HOS cells were transfected with pc-HMGA1 or pcDNA3.1, whereas *HMGA1* siRNA or NC siRNA was introduced into miR-758-downregulated U2OS cells. A. HMGA1 protein level was analyzed in HOS and U2OS cells. **P* < 0.05 vs. miR-NC. ***P* < 0.05 vs. miR-758 mimics + pcDNA3.1. #*P* < 0.05 vs. NC inhibitor. ##*P* < 0.05 vs. miR-758 inhibitor + NC siRNA. B-F. MTT assay, clonogenic survival assay, flow cytometry analysis, and transwell assays were performed to determine proliferation, colony formation, apoptosis, migration, and invasion of HOS and U2OS cells treated as mentioned above, respectively. **P* < 0.05 vs. miR-NC. ***P* < 0.05 vs. miR-758 mimics + pcDNA3.1. #*P* < 0.05 vs. NC inhibitor. ##*P* < 0.05 vs. miR-758 inhibitor + NC siRNA.

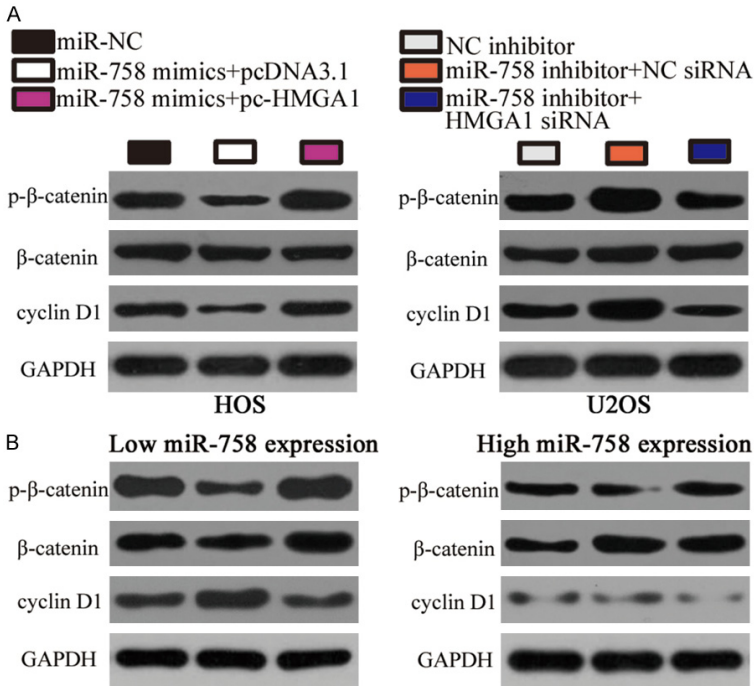

Figure 6. miR-758 inhibits the activation of the Wnt/β-catenin pathway in OS in vitro and in vivo. A. HOS cells were co-transfected with miR-758 mimics and pc-HMGA1 or pcDNA3.1. U2OS cells were co-transfected with miR-758 inhibitor and *HMGA1* siRNA or NC siRNA. Western blot analysis was performed to detect p-β-catenin, β-catenin, and cyclin D1 protein levels 72 h after transfection. B. The protein levels of p-β-catenin, β-catenin and cyclin D1 in OS tissues was detected through western blot analysis.

restricted when *HMGA1* expression was silenced (**Figure 4B** and **4C**, *P* < 0.05). Furthermore, the effect of miR-758 on OS cell apoptosis was determined using flow cytometry analysis. As shown in **Figure 4D**, apoptosis was significantly induced in HOS and U2OS cells transfected with *HMGA1* siRNA (*P* < 0.05). In addition, transwell assays revealed that *HMGA1* inhibition attenuated the migratory (**Figure 4E**, *P* < 0.05) and invasive (**Figure 4F**, *P* < 0.05) abilities of HOS and U2OS cells. These observations demonstrated that *HMGA1* knockdown simulated the anti-tumor effects induced by miR-758 upregulation, further suggesting that *HMGA1* is a downstream mediator of miR-758 in OS.

Restoration of HMGA1 expression counteracts the anti-cancer effects of miR-758 on OS cells

To further demonstrate that *HMGA1* mediated the tumor-suppressive roles of miR-758 in OS cells, a series of rescue experiments were performed in which *HMGA1* expression was recovered in HOS and U2OS cells. To achieve this, miR-758 mimics-transfected HOS cells were further co-transfected with pcDNA3.1-HMGA1 (pc-HMGA1) or empty pcDNA3.1 plasmid, whereas *HMGA1* siRNA or NC siRNA was introduced into miR-758 inhibitor-transfected U2OS cells. Western blot analysis confirmed that the *HMGA1* downregulation in HOS cells and upregulation in U2OS cells was achieved after co-transfection with pc-HMGA1 and *HMGA1* siRNA, respectively (**Figure 5A**, *P* < 0.05). Furthermore, restoration of *HMGA1* expression partially attenuated miR-758-mediated effects on HOS and U2OS cell proliferation (**Figure 5B**, *P* < 0.05), colony formation ability (**Figure 5C**, *P* < 0.05), apoptosis (**Figure 5D**, *P* < 0.05), migration (**Figure 5E**, *P* < 0.05), and invasion (**Figure 5F**, *P* < 0.05) in vitro. Collectively, these results demonstrated that *HMGA1* partially mediates the effects of miR-758 on the aggressive phenotypes of OS cells.

miR-758 inhibits the activation of the Wnt/β-catenin pathway in OS cells

Previous reports have shown that *HMGA1* is involved in the Wnt/β-catenin pathway in multiple human cancers [21, 26, 27]. Hence, we

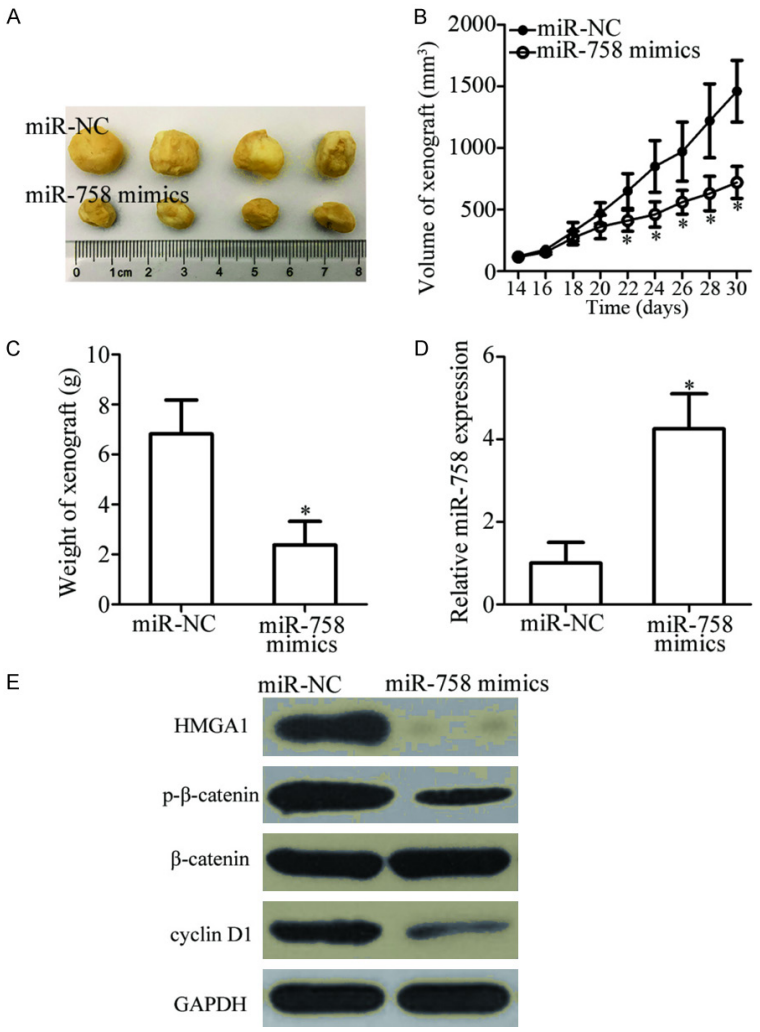

Figure 7. miR-758 inhibits OS tumor growth in vivo. HOS cells were transfected with miR-758 mimics or miR-NC. The transfected cells were collected and subcutaneously injected into the flanks of nude mice after 24 h. A. Representative images of the tumor xenografts in miR-758 mimics and miR-NC groups. B. After 2 weeks, the volume of the tumor xenografts was detected and calculated using the following formula: Volume (mm^3) = Width^2 (mm^2) * Length (mm)/2. *P < 0.05 vs. miR-NC. C. Nude mice were sacrificed one month after the inoculation. The tumor xenografts were excised and weighed. *P < 0.05 vs. miR-NC. D. Total RNA was isolated from xenografts derived from miR-758 mimics- or miR-NC-transfected HOS cells, and miR-758 expression was determined. *P < 0.05 vs. miR-NC. E. Western blot analysis was performed to determine HMGA1, p-β-catenin, β-catenin, and cyclin D1 protein levels in the xenografts.

next investigated whether miR-758 deactivated the Wnt/β-catenin pathway in OS cells by inhibiting *HMGA1* expression. Western blot analysis indicated that miR-758 upregulation decreased the protein levels of p-β-catenin and cyclin D1 in HOS cells, whereas miR-758 knockdown increased p-β-catenin and cyclin D1 levels in H2OS cells. However, the level of total β-catenin in both HOS and U2OS cells was unaffected. In addition, miR-758-induced changes in p-β-catenin and cyclin D1 protein levels were restored in HOS and U2OS cells in which *HMGA1* expression had been recovered (**Figure 6A**). We further determined the expression of p-β-catenin, β-catenin, and cyclin D1 in OS tissues from low and high miR-758 expression groups. Consistently, the levels of p-β-catenin and cyclin D1 in high miR-758 expression group were significantly lower than those in low miR-758 expression group (**Figure 6B**). These results suggest that miR-758 inhibits the activation of the Wnt/β-catenin pathway in OS, which may partially explain the mechanism underlying the functions of miR-758.

miR-758 hinders the tumorous growth of OS cells in vivo

Xenograft assay was performed to assess the effect of miR-758 on OS cell growth in vivo. A subcutaneous xenograft model was generated by injecting miR-758 mimics- or miR-NC-transfected HOS cells into nude mice. An obvious suppression in xenograft tumor volume (**Figure 7A** and **7B**, P < 0.05) and weight (**Figure 7C**, P < 0.05) was observed in the miR-758 mimics group. In addition, upregulation of miR-758 expression by miR-758 mimics transfection was verified in the xenograft using RT-qPCR (**Figure 7D**, P < 0.05). Furthermore, western blot analysis revealed that *HMGA1*, p-β-catenin, and cyclin D1 protein levels were reduced in the tumor xenograft derived from miR-758 mimics-transfected HOS cells (**Figure 7E**). These results showed that miR-758 hindered tumor growth in OS in vivo by regulating the HMGA1/Wnt/β-catenin pathway.

Discussion

Increasing evidence indicates that miRNAs are frequently dysregulated in OS and are implicated in the oncogenesis and development of OS [28-30]. The mechanism underlying OS formation and progression is critical for predicting prognosis and identifying therapeutic targets for patients with OS [31]. Hence, an in-depth investigation of miRNAs with aberrant expression and their roles in OS is crucial for developing novel prognostic biomarkers and therapeutic targets. In this study, for the first time, we analyzed miR-758 expression in OS tissues and cells and evaluated its clinical significance. In particular, the function and mechanism of miR-758 action in OS were investigated. Our results suggested that miR-758 may function as a tumor suppressive miRNA in OS both in vitro and in vivo by directly targeting *HMGA1* and regulating the Wnt/β-catenin pathway.

miR-758 is downregulated in non-small cell lung cancer tissues, which correlates with tumor-necrosis-metastases stage. Non-small cell lung cancer patients with low miR-758 expression have shorter overall survival than patients with high miR-758 expression [16]. miR-758 expression is also low in cervical cancer tissues, which is related to infiltration and invasion of cervical cancer [17]. In addition, miR-758 is expressed at low levels in retinoblastoma [18] and hepatocellular carcinoma [19]. However, the expression pattern of miR-758 in OS remains unclear. Herein, we used RT-qPCR to detect miR-758 expression, and observed that miR-758 was poorly expressed in OS tissues and cell lines. miR-758 expression correlated with the tumor size, clinical stage, and distant metastasis of patients with OS. Furthermore, OS patients with low miR-758 level exhibited poorer overall survival and worse disease-free survival compared to patients with high miR-758 level. These findings suggest that miR-758 might be an effective biomarker for the diagnosis and prognosis of specific human cancer types.

miR-758 plays tumor suppressive roles. For instance, miR-758 overexpression has been shown to inhibit proliferation, migration, and invasion, and promote apoptosis of retinoblastoma cells in vitro [18]. Exogenous miR-758 expression restricts cell growth and metastasis in hepatocellular carcinoma in vitro [19]. Nevertheless, the detailed roles of miR-758 in OS are still poorly understood. Our study showed that miR-758 exerted tumor-suppressing roles in OS cells by regulating cell growth and metastasis in vitro and tumor growth in vivo. These observations suggest that miR-758 might serve as a promising target for the treatment of patients with the above-mentioned cancer types.

Four human genes, namely, matrix extracellular phosphoglycoprotein in cervical cancer [17], paired box protein 6 in retinoblastoma [18], and mouse double minute 2 homolog and mammalian target of rapamycin in hepatocellular carcinoma [19] have been validated as the direct targets of miR-758. *HMGA1*, a member of the HMGA protein family, was demonstrated to be a novel direct target of miR-758 in OS. *HMGA1* regulates chromatin structure by directly binding to the A/T-rich DNA sequences located in the promoter and enhancer regions of multiple human genes [32]. *HMGA1* expression has been reported to be upregulated in various human cancers, including colorectal cancer [21], lung cancer [22], breast cancer [23], and glioma [24]. *HMGA1* expression is upregulated in OS tissues and exerts crucial roles in OS formation and progression [25]. *HMGA1* is able to activate the Wnt/β-catenin pathway, which is central to carcinogenesis [21, 26, 27]. Wnt/β-catenin signaling is implicated in the regulation of aggressive behaviors of OS cells, including cell proliferation, cycle, apoptosis, metastasis, epithelial-mesenchymal transition, and chemoresistance [33-36]. More importantly, recent studies have documented that targeting the Wnt/β-catenin pathway may be a potential therapeutic strategy for the treatment of patients with OS [33, 34]. In this study, we also demonstrated that the miR-758/HMGA1 axis inhibited the aggressive phenotypes of OS cells both in vitro and in vivo, and the Wnt/β-catenin pathway was deactivated in this process. Accordingly, *HMGA1* inhibition- or miR-758 restoration-mediated deactivation of the Wnt/β-catenin pathway might be a valuable approach for treating patients with OS.

In conclusion, miR-758 expression was downregulated in OS tissues and cells. Its downregulation was correlated with malignant clinical features and predicted poor survival of patients

with OS. Furthermore, miR-758 suppressed the progression and development of OS in vitro and in vivo by directly targeting *HMGA1* and regulating the Wnt/β-catenin pathway. Identification and characterization of the specific roles of miR-758 in OS might be beneficial for understanding the molecular mechanisms underlying OS pathogenesis, as well as for developing effective therapeutic targets for OS treatment.

Disclosure of conflict of interest

None.

Address correspondence to: Jia Ren, Department of Emergency, The First Affiliated Hospital of Zhengzhou University, No. 1 Jianshe East Road, Zhengzhou Henan 450052, P. R. China. E-mail: emergency_renjia@163.com

References

[1] Yang J and Zhang W. New molecular insights into osteosarcoma targeted therapy. Curr Opin Oncol 2013; 25: 398-406.

[2] Berman SD, Calo E, Landman AS, Danielian PS, Miller ES, West JC, Fonhoue BD, Caron A, Bronson R, Bouxsein ML, Mukherjee S and Lees JA. Metastatic osteosarcoma induced by inactivation of Rb and p53 in the osteoblast lineage. Proc Natl Acad Sci U S A 2008; 105: 11851-11856.

[3] Ferrari S and Serra M. An update on chemotherapy for osteosarcoma. Expert Opin Pharmacother 2015; 16: 2727-2736.

[4] Mirabello L, Troisi RJ and Savage SA. Osteosarcoma incidence and survival rates from 1973 to 2004: data from the surveillance, epidemiology, and end results program. Cancer 2009; 115: 1531-1543.

[5] Gorlick R and Khanna C. Osteosarcoma. J Bone Miner Res 2010; 25: 683-691.

[6] Ottaviani G and Jaffe N. The etiology of osteosarcoma. Cancer Treat Res 2009; 152: 15-32.

[7] Bartel DP. MicroRNAs: genomics, biogenesis, mechanism, and function. Cell 2004; 116: 281-297.

[8] Chen K and Rajewsky N. The evolution of gene regulation by transcription factors and microRNAs. Nat Rev Genet 2007; 8: 93-103.

[9] Sun K and Lai EC. Adult-specific functions of animal microRNAs. Nat Rev Genet 2013; 14: 535-548.

[10] Griffiths-Jones S, Grocock RJ, van Dongen S, Bateman A and Enright AJ. miRBase: microRNA sequences, targets and gene nomenclature. Nucleic Acids Res 2006; 34: D140-144.

[11] Kim YH, Goh TS, Lee CS, Oh SO, Kim JI, Jeung SH and Pak K. Prognostic value of microRNAs in osteosarcoma: a meta-analysis. Oncotarget 2017; 8: 8726-8737.

[12] Wang W, Guo Z, Yu H and Fan L. MiR-216b inhibits osteosarcoma cell proliferation, migration, and invasion by targeting Forkhead Box M1. J Cell Biochem 2018; [Epub ahead of print].

[13] Tian ZG, Zhuang Y, Jin Z, Zhou F, Zhu LF and Shen PC. MicroRNA-337-5p participates in the development and progression of osteosarcoma via ERBB, MAPK and VEGF pathways. Eur Rev Med Pharmacol Sci 2018; 22: 5460-5470.

[14] Wang L, Hu K and Chao Y. MicroRNA-1301 inhibits migration and invasion of osteosarcoma cells by targeting BCL9. Gene 2018; 679: 100-107.

[15] Kushlinskii NE, Fridman MV and Braga EA. Molecular mechanisms and microRNAs in osteosarcoma pathogenesis. Biochemistry (Mosc) 2016; 81: 315-328.

[16] Wang S and Jiang M. The long non-coding RNA-DANCR exerts oncogenic functions in non-small cell lung cancer via miR-758-3p. Biomed Pharmacother 2018; 103: 94-100.

[17] Meng X, Zhao Y, Wang J, Gao Z, Geng Q and Liu X. Regulatory roles of miRNA-758 and matrix extracellular phosphoglycoprotein in cervical cancer. Exp Ther Med 2017; 14: 2789-2794.

[18] Li J and You X. MicroRNA758 inhibits malignant progression of retinoblastoma by directly targeting PAX6. Oncol Rep 2018; 40: 1777-1786.

[19] Jiang D, Cho W, Li Z, Xu X, Qu Y, Jiang Z, Guo L and Xu G. MiR-758-3p suppresses proliferation, migration and invasion of hepatocellular carcinoma cells via targeting MDM2 and mTOR. Biomed Pharmacother 2017; 96: 535-544.

[20] Livak KJ and Schmittgen TD. Analysis of relative gene expression data using real-time quantitative PCR and the 2(-Delta Delta C(T)) Method. Methods 2001; 25: 402-408.

[21] Xing J, Cao G and Fu C. HMGA1 interacts with beta-catenin to positively regulate Wnt/beta-catenin signaling in colorectal cancer cells. Pathol Oncol Res 2014; 20: 847-851.

[22] Zhang Z, Wang Q, Chen F and Liu J. Elevated expression of HMGA1 correlates with the malignant status and prognosis of non-small cell lung cancer. Tumour Biol 2015; 36: 1213-1219.

[23] Qi C, Cao J, Li M, Liang C, He Y, Li Y, Li J, Zheng X, Wang L and Wei B. HMGA1 overexpression is associated with the malignant status and progression of breast cancer. Anat Rec (Hoboken) 2018; 301: 1061-1067.

[24] Pang B, Fan H, Zhang IY, Liu B, Feng B, Meng L, Zhang R, Sadeghi S, Guo H and Pang Q. HMGA1 expression in human gliomas and its correlation with tumor proliferation, invasion and angiogenesis. J Neurooncol 2012; 106: 543-549.
[25] Xu G, Wang J, Jia Y, Shen F, Han W and Kang Y. MiR-142-3p functions as a potential tumor suppressor in human osteosarcoma by targeting HMGA1. Cell Physiol Biochem 2014; 33: 1329-1339.
[26] Han X, Cao Y, Wang K and Zhu G. HMGA1 facilitates tumor progression through regulating Wnt/beta-catenin pathway in endometrial cancer. Biomed Pharmacother 2016; 82: 312-318.
[27] Akaboshi S, Watanabe S, Hino Y, Sekita Y, Xi Y, Araki K, Yamamura K, Oshima M, Ito T, Baba H and Nakao M. HMGA1 is induced by Wnt/beta-catenin pathway and maintains cell proliferation in gastric cancer. Am J Pathol 2009; 175: 1675-1685.
[28] Wang C, Jing J and Cheng L. Emerging roles of non-coding RNAs in the pathogenesis, diagnosis and prognosis of osteosarcoma. Invest New Drugs 2018; 36: 1116-1132.
[29] Sampson VB, Yoo S, Kumar A, Vetter NS and Kolb EA. MicroRNAs and potential targets in osteosarcoma: review. Front Pediatr 2015; 3: 69.
[30] Chang L, Shrestha S, LaChaud G, Scott MA and James AW. Review of microRNA in osteosarcoma and chondrosarcoma. Med Oncol 2015; 32: 613.
[31] Varshney J and Subramanian S. MicroRNAs as potential target in human bone and soft tissue sarcoma therapeutics. Front Mol Biosci 2015; 2: 31.
[32] Benecke AG and Eilebrecht S. RNA-mediated regulation of HMGA1 function. Biomolecules 2015; 5: 943-957.
[33] Huang W, Zheng X, Yang X and Fan S. Stimulation of osteogenic differentiation by saikosaponin-a in bone marrow stromal cells via WNT/beta-catenin pathway. Calcif Tissue Int 2017; 100: 392-401.
[34] Lin CH, Ji T, Chen CF and Hoang BH. Wnt signaling in osteosarcoma. Adv Exp Med Biol 2014; 804: 33-45.
[35] Li X, Lu Q, Xie W, Wang Y and Wang G. Antitumor effects of triptolide on angiogenesis and cell apoptosis in osteosarcoma cells by inducing autophagy via repressing Wnt/beta-Catenin signaling. Biochem Biophys Res Commun 2018; 496: 443-449.
[36] Scholten DJ 2nd, Timmer CM, Peacock JD, Pelle DW, Williams BO and Steensma MR. Down regulation of Wnt signaling mitigates hypoxia-induced chemoresistance in human osteosarcoma cells. PLoS One 2014; 9: e111431.